



Technical note

3D surface form error evaluation using high definition metrology



Meng Wang*, Lifeng Xi, Shichang Du

State Key Laboratory of Mechanical System and Vibration, Department of Industrial Engineering & Logistics Management, Shanghai Jiao Tong University, Shanghai 200240, PR China

ARTICLE INFO

Article history:

Received 12 March 2013
Received in revised form 26 June 2013
Accepted 27 August 2013
Available online 12 September 2013

Keywords:

High definition metrology
3D surface form error
Flatness
3D surface texture

ABSTRACT

This paper presents an approach to evaluate 3D surface form error of machined surface using high definition metrology that can measure millions of data points representing the entire surface. A data preprocessing method was developed to convert the mass data into a height-encoded and position-maintained gray image. With the converted image, a modified gray level co-occurrence matrix method was adopted to extract 3D surface form error characteristics, including entropy, contrast and correlation. Entropy measures the randomness of surface height distribution. Contrast indicates the degree of surface local deviations. Correlation could be used to identify different machining techniques. These characteristics can be used with flatness together to evaluate 3D surface form error of large complex surface.

© 2013 Elsevier Inc. All rights reserved.

1. Introduction

During the last decade, the evaluation of surface geometric qualities (surface texture and surface form) gradually changes from 2D profile to 3D areal characterization [1]. For example, the evaluation of surface texture has extended from roughness and waviness to 3D surface texture, from 2D-Motif to 3D-Motif, and from 2D material ratio curve to 3D material ratio curve. However, compared with the remarkable evaluation methods on 3D surface texture, there is limited research on 3D surface form error. In general, surface form error is evaluated using surface flatness measured by coordinate measuring machines (CMMs). As CMM measures only a few scattered points or profiles due to economic constraints [2], it cannot sample high-density points describing 3D surface form error in industrial application. Recently, non-contact high definition metrology (HDM) has been adopted for its 3D inspection of the entire surface as HDM can generate a surface height map of millions of data points within seconds [3]. HDM provides possibility to evaluate 3D surface form error in many aspects besides surface flatness. Therefore, the purpose of this research is to develop a proper method to evaluate the 3D surface form error using HDM data.

To begin with, we first discuss the scope of 3D surface form error. In the authors' point of view, 3D surface form error describes relatively long-wavelength deviations from a 3D areal characterization of an entire machined surface. According to the authors'

definition, there are differences and similarities between 3D surface form error and 2D surface texture, 3D surface texture, as well as flatness measured by CMM. These four types of surface geometric qualities are classified by a two-dimensional coordinate system (Fig. 1). The horizontal coordinate is the lateral resolution of the corresponding measurement techniques, and the vertical coordinate is the metrology dimension. Therefore, 3D surface form error differs from flatness measured by CMM in metrology dimension and 3D surface texture in lateral resolution. As for similarities, 3D surface form error has the same level of lateral resolution with surface flatness and has the same metrology dimension with 3D surface texture.

As both 3D surface texture and 3D surface form error are based on 3D areal measurement, the evaluation methods for 3D surface texture can be adopted to evaluate 3D surface form error to a certain degree. 3D surface texture is typically measured by areal-topography methods (ATM) such as phase-shifting interferometry, coherence scanning interferometry, and atomic force microscopy [4]. A series of successful studies such as "Birmingham 14 parameters" [5–8] and international standards on 3D surface texture [9] were achieved. Among these parameters, certain 3D surface texture parameters such as height parameters in ISO 25178-Part 2 [9] can be extended to evaluate HDM data. However, other 3D surface texture parameters are not fit to evaluate HDM data. There are two reasons. The first reason is the measurement continuity. ATM usually measures a simple square area that has no holes or empty zones. Therefore, ATM data are continuously sampled, so the 3D surface texture parameters can be calculated directly. On the contrary, HDM measures the entire surface probably with many holes and empty zones. For instance, engine block faces measured by HDM in Fig. 1 have cylinder holes, bolt holes and cooling

* Corresponding author. Tel.: +86 2134201738.

E-mail address: mwang@sjtu.edu.cn (M. Wang).

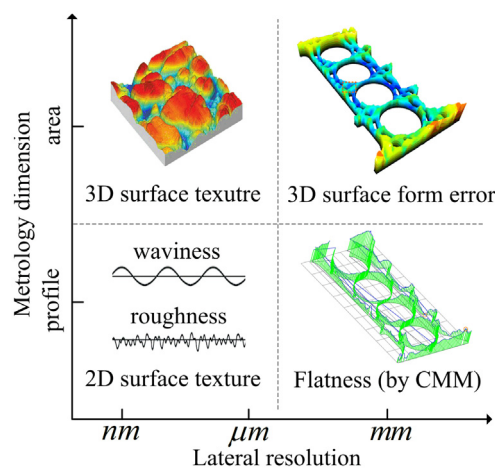


Fig. 1. Classification of surface geometrical qualities.

holes. Therefore, HDM data are not continuously measured, so the 3D surface form error cannot be analyzed directly by using 3D surface texture methods such as 3D frequency filtering. The second reason is the lateral resolution or deviation wavelength between HDM and ATM. ATM measures typically a selected area with an edge of several millimeters with lateral resolution at the scale of micrometer or even nanometer. However, HDM measures the entire surface with an edge of several hundred millimeters at sub-millimeter resolution. Therefore, 3D surface texture parameters, which focus on the short-wavelength, high-frequency deviation of local regions, are not designed for evaluating the long-wavelength, low-frequency deviation of the entire surface. The above two reasons also explain why we assign HDM measurement to the scope of 3D surface form error instead of 3D surface texture.

Recently published research has adopted some characteristic extraction techniques using HDM data for various applications [10–13]. However, the extracted characteristics are inadequate for evaluating 3D surface form error. Because characteristics for surface form error evaluation must have engineering meaning whereas those for surface classification and surface partition do not have to. In a short summary, 3D surface form error information has not been mined and analyzed sufficiently using HDM data.

The evaluation of 3D surface form error should focus on two problems. The first problem is to process raw HDM data into a suitable data type for evaluating the entire surface that has holes or empty zones. The second problem is to extract meaningful characteristics describing 3D surface form error. In this research, an evaluation method for 3D surface form error is proposed to tackle the two problems. First, a HDM data preprocessing method is proposed to convert HMD data into a height-encoded gray image containing all the height and spatial information of entire surface. Gray values and positions of pixels in the image are assigned to height deviations and spatial positions of the measurement points of the surface, respectively. Second, a modified GLCM method is developed to evaluate 3D surface form error of machined surface with complex geometry, which eliminates the influence of the empty zone of the surface. From the modified GLCM, characteristics such as entropy, contrast, and correlation are calculated. These characteristics having engineering meaning complement 3D surface form error evaluation.

The remainder of this paper is organized as follows: Section 2 describes an evaluation method for 3D surface form error, including the HDM data preprocessing method and the modified GLCM method. Section 3 presents a case study to show the effectiveness of the proposed 3D surface form evaluation method in industrial

use. Section 4 draws the conclusions and discusses the future research.

2. Proposed method

The proposed method for 3D surface form error evaluation includes two parts: a HDM data preprocessing method and a modified GLCM method, which are illustrated in Sections 2.1 and 2.2, respectively.

2.1. HDM data preprocessing method

In this section, a HDM data preprocessing method is proposed to convert HDM data into a height-encoded and position-maintained gray image. The height information (Z coordinates of HDM data) is converted to pixel gray intensities, and the spatial information (X and Y coordinates) is converted to pixel index. The converted gray image reduces the data size to about one third of the size of raw HDM data and serves as a suitable data type for further analysis. Fig. 2 shows the four steps of the HDM data preprocessing method, including HDM data alignment, grid generation, grayscale converting, and empty zone removing.

The first step is obtaining the orthogonal height deviations from raw HDM data $[x_i, y_i, z_i]$, where $i = 1, 2, \dots, N$ is the number of the measurement points. The raw HDM data are relative to the reference plane of HDM. Unless the measured surface is perfectly aligned with the reference plane, raw data will be tilted with respect to the measured surface. A least square plane P is fitted to acquire the nominal measured surface:

$$P : ax + by + c - z = 0 \quad (1)$$

The original coordinates $[x_i, y_i, z_i]$ can be transformed to new coordinates $[X_i, Y_i, Z_i]$ on the fitted plane P . The orthogonal height deviation Z_i is calculated by:

$$Z_i = \frac{z_i - ax_i - by_i - c}{\sqrt{1 + a^2 + b^2}} \quad (2)$$

The second step is generating a regular grid of height deviation Z_i . A continuous surface is interpolated using coordinates $[X_i, Y_i, Z_i]$ by Delaunay triangulation [14]. From the interpolated surface, a

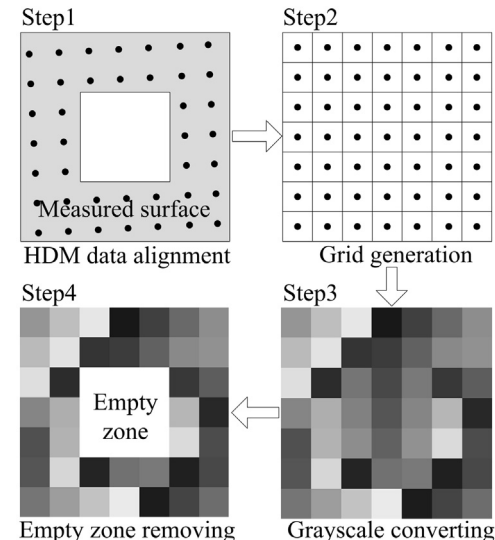


Fig. 2. HDM data preprocessing method.

two-dimensional grid matrix $Z(m, n)$ is resampled. The index m and n are calculated as follows, given the resampling interval l :

$$\begin{aligned} m &= \frac{X_i - X_{\min}}{l} \\ n &= \frac{Y_i - Y_{\min}}{l} \end{aligned} \quad (3)$$

The grid matrix $Z(m, n)$ stores both height information and spatial information of the entire surface: the value of $Z(m, n)$ contains vertical deviation Z_i and the index m and n represent the spatial information X_i and Y_i .

The third step is converting the grid matrix $Z(m, n)$ into a gray image $G(m, n)$. Each element of the grid matrix is assigned a pixel of the image. The spatial index m and n in the grid matrix are correlated to the positions of pixels in the image. The vertical deviations in the grid matrix $Z(m, n)$ are scaled to pixel gray intensity $G(m, n)$ with gray interval from 0 (black) to 255 (white). Gray intensity $G(m, n)$ is calculated as:

$$G(m, n) = \left[\frac{Z(m, n) - S_L}{S_U - S_L} \times 255 \right] \quad (4)$$

where $[*]$ is the round operator, and S_L, S_U are the lower and upper specification. S_L and S_U should remain unchanged for the same type of parts for comparison purpose.

The last step is removing the empty zone of the gray image $G(m, n)$. As the empty zone is also interpolated in the second step, it should be removed by comparing the inner and outer edge of the measured surface. The final gray image $I(m, n)$ is achieved by multiplying $G(m, n)$ with a selective parameter $\delta(m, n)$, which decides whether pixels belong to the surface or not:

$$I(m, n) = G(m, n) \cdot \delta(m, n) \quad (5)$$

$$\delta(m, n) = \begin{cases} 0, & \text{if } \sqrt{(X_{\min} + ml - X_i)^2 + (Y_{\min} + nl - Y_i)^2} > \varepsilon, \forall i = 1, \dots, N \\ 1, & \text{otherwise} \end{cases} \quad (6)$$

where ε is the selective margin.

Through the above four steps, HDM data is converted to a gray image by establishing correspondence relationship between coordinates $[x_i y_i z_i]$ and pixels in gray image $I(m, n)$. Then the gray image $I(m, n)$ that contains all the height and spatial information of HDM data can be analyzed by image-analysis techniques directly for 3D surface form error evaluation purpose.

2.2. Modified GLCM method

In this section, a modified gray level co-occurrence matrix (GLCM) is adopted to evaluate 3D surface form error using the converted gray image. GLCM describes how frequent one gray level appears in a specified relationship to another gray level of the image [15], which is a successful image analysis technique to study textural features. Given the gray image $I(x, y)$, the normalized co-occurrence frequencies $p(i, j)$ between gray level i and j are defined as:

$$p(i, j) = \frac{P(i, j)}{\sum_{i=1}^{N_g} \sum_{j=1}^{N_g} P(i, j)} \quad (7)$$

$$\begin{aligned} P(i, j) &= \#\{I(x_1, y_1) = i, I(x_2, y_2) = j, x_2 = x_1 + d \cos \theta, \\ y_2 &= y_1 + d \sin \theta\}, i \neq 0, j \neq 0 \end{aligned} \quad (8)$$

where N_g is the number of gray levels, i and j are corresponding gray levels of pixels $I(x_1, y_1)$ and $I(x_2, y_2)$ with a distance d and an angle θ , and $\#$ denotes the number of pixel pairs satisfying the conditions. As computing GLCM for all distances d and angles θ would require a lot of calculation, GLCM calculated for angles quantized to 45° and

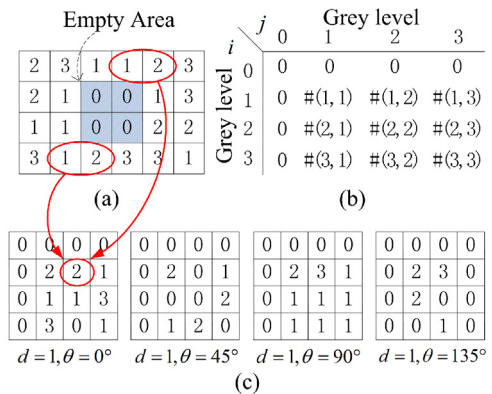


Fig. 3. Calculating modified GLCM: (a) a gray image of machined surface, (b) the general form of GLCM with condition $i \neq 0, j \neq 0$, (c) four GLCMs of $d=1$ and $\theta=0^\circ, 45^\circ, 90^\circ, 135^\circ$.

distance of one or two pixels are suggested [15]. The dimension of $p(i, j)$ is equal to the gray levels N_g in the image. For example, if the gray levels are between 0 and 255, the size of the $p(i, j)$ will be 256 by 256. Note that the calculated GLCMs vary for different numbers of gray level N_g . Along with the decrease of gray levels from 256, the spatial and height information will lose. Therefore, gray levels equal to 256 is suggested to make most of the information from the converted gray image.

Unlike the traditional definition of GLCM, a further condition $i \neq 0, j \neq 0$ is added when calculating GLCM of machined surfaces. This condition ensures that pixel pairs with either one pixel equal to zero are not counted in calculating GLCM. Because the pixel values of the measured surface are usually at the middle range of the gray interval [0 255], only the empty zone can have zero values. Therefore, pixel pairs with one zero-pixel represent the edge of the surface and those with two zero-pixels represent the empty zone, which should be eliminated when evaluating 3D surface form information.

Fig. 3 shows an example of how to calculate the modified GLCM of a 4-by-6 gray image. The image with zero pixels in the middle is a simple illustration of a machined surface with a hole (**Fig. 3a**). The hole will look like a smooth circle in the image provided enough pixels especially millions of HDM data points. As the gray level of the image is 4, the dimension of corresponding GLCM is 4-by-4. **Fig. 3b** shows the general form of the modified GLCM, where $\#$ denotes the number of pixel pairs satisfying the conditions. Considering the additional condition $i \neq 0, j \neq 0$, the pixel pairs $(0, 0), (0, j)$, and $(i, 0)$ are not counted in the GLCM to eliminate the information of the hole. Four GLCMs for a distance equal to one and an angle equal to $0^\circ, 45^\circ, 90^\circ, 135^\circ$ are shown in **Fig. 3c**. More specifically, the value of element $(1, 2)$ in the GLCM of $d=1, \theta=0^\circ$ is 2 because horizontally adjacent pixels with the values 1 and 2 appear twice. Continuing this procedure will fill in the values in GLCM.

From the modified GLCM, three uncorrelated features, entropy, contrast, and correlation, are calculated as follows:

$$\text{entropy} = - \sum_i \sum_j p(i, j) \log(p(i, j)) \quad (9)$$

$$\text{contrast} = \sum_{n=0}^{N_g-1} (i-j)^2 \left\{ \sum_{i=1}^{N_g} \sum_{j=1}^{N_g} p(i, j) \right\} \quad (10)$$

$$\text{correlation} = \frac{\sum_i \sum_j (ij)p(i, j) - \mu_x \mu_y}{\sigma_x \sigma_y} \quad (11)$$

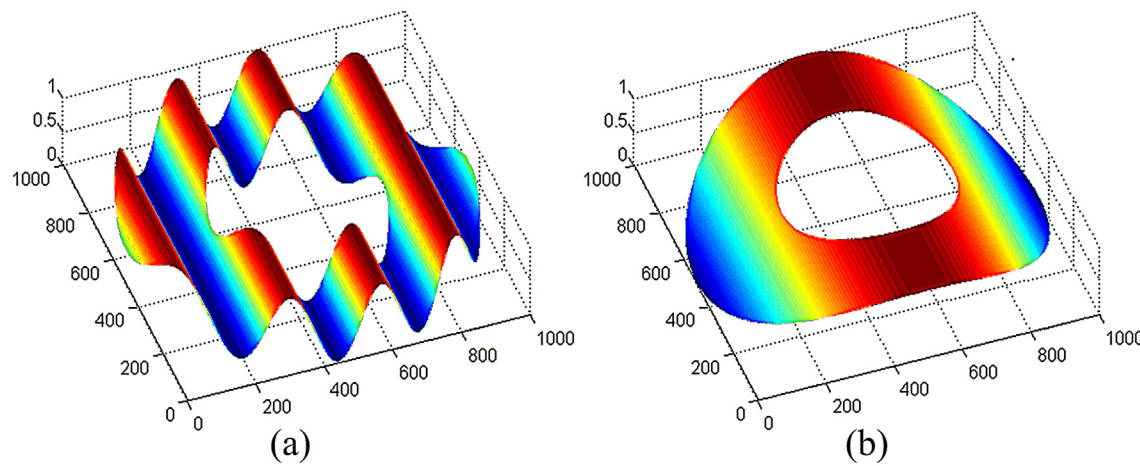


Fig. 4. Simulated plates with the same flatness: (a) contrast = 5.11, entropy = 6.35, (b) contrast = 0.54, entropy = 6.30.

where p_x and p_y are marginal probability of $p(i, j)$, and μ_x , μ_y , σ_x , and σ_y are the mean and standard deviation of p_x and p_y .

Entropy evaluates the randomness of the surface height distribution of the measured points. If the height of the measured points is regularly distributed within a narrow range, entropy will be small. If the height of the measured points is randomly distributed, entropy will be large. Specifically, entropy will be zero for a surface of which the measured points have the same height, and entropy will reach its maximum for a surface with completely random height distribution.

Contrast measures the amount of local surface height difference between a pixel and its neighbor over the whole image. Since the height difference $i - j$ is magnified to $(i - j)^2$, contrast is sensitive to the local height difference. Therefore, contrast can be used to distinguish whether surface flatness is caused by global variation or local variation. For example, suppose two surfaces A (Fig. 4a) and B (Fig. 4b) with same flatness but caused by local variations and global trend, respectively. As the local height difference of surface A is greater than that of surface B, contrast of surface A is greater than contrast of surface B. In a similar perspective, low flatness is a sufficient, but not necessary condition to keep low contrast [16].

Correlation reflects the degree of how correlated a pixel to another pixel in certain direction and distance. It indicates directionality of surface height distribution in the row or column. High correlation implies significant directionality of the surface in that direction and vice versa. Correlation could be used to distinguish surfaces machined by different processing techniques.

These characteristics, entropy, contrast, and correlation, can be used with flatness together to evaluate 3D surface form error measured by HDM. Through 3D surface form error evaluation, engineers can better understand quality of machined surface from various angles and making due adjustment of the machining process. Moreover, these characteristics also provide possibility to evaluate certain 3D form error related properties, for example, the mechanical sealing property for large sealing surfaces.

3. Case study

In this section, a case study on engine block faces was presented to illustrate the evaluation of 3D surface form error using HDM data. The extracted 3D form error characteristics were compared with the flatness, and the usefulness of the proposed method was discussed.

3.1. Experimental conditions

The experimental parts were engine blocks, the face of which is a major sealing surface in automotive powertrain. The material of the engine block is Cast Iron FC250. The milling process was carried in an EX-CELL-O Machining Center using a CBN milling cutter with a diameter of 200 mm. Quaker 370 KLG cutting fluid was used. The cutting speed was 816.4 m/min, the depth of cut was 0.5 mm, and feed rate was 3360 mm/min. Ten engine blocks were sampled from different production lines and measured by a 3D laser holographic system (ShaPix® Surface Detective™, Ann Arbor, MI) with lateral resolution 0.15 mm. About 0.8 million points on an area of 320 mm × 160 mm were acquired for each engine block. The flatness of the ten engine blocks was calculated using the least square method. The numbers of engine blocks were rearranged in an ascending order of flatness: the engine block with smallest flatness is marked as Block1 and that with largest flatness is marked as Block 10. However, Block 10 was removed as its flatness was out of flatness tolerance (50 µm). Flatness of the rest nine blocks is shown in Fig. 5.

3.2. Experimental results

The HDM data preprocessing method in Section 2.1 was applied to convert HDM data into gray images. The interpolation interval l was 0.2 mm. The lower and upper specification S_L and S_U were assigned from −30 µm to 30 µm to 256 gray levels of the image. Fig. 6 shows a converted gray scale image of the engine block face.

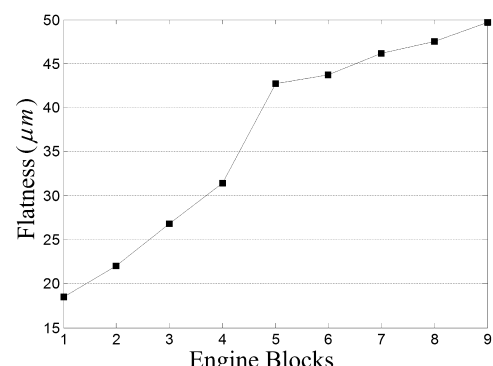


Fig. 5. Engine blocks rearranged in an ascending order of flatness.

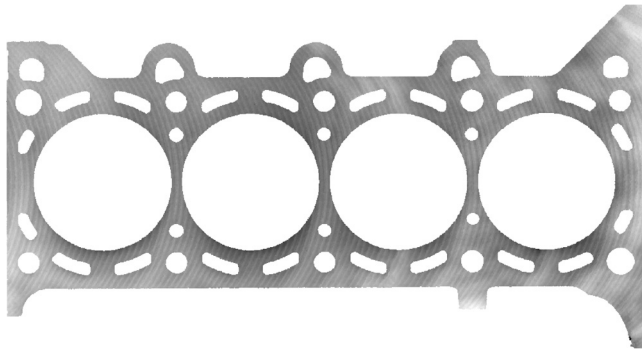


Fig. 6. A gray image of engine block face.

The GMCMs of the nine blocks were calculated using the modified GLCM method in Section 2.2 with pixel distance equal to 1, 2, 3, 4, and 5 and the angles equal to 0° , 45° , 90° , 135° . Fig. 7 shows GLCMs of Block 1 to Block 9 with pixel distance of 1. We find that the non-zero elements of the GLCMs are centered near the matrix diagonal; the length of matrix diagonal is longer for the surface with

larger flatness. Other research pointed out that the surface flatness is inverse propositional to the width of the matrix diagonal [17,18], which is also correct for large pixel distance.

Entropy, contrast and correlation were calculated as an average of GLCM in four directions for pixel distance d equal to 1, 2, 3, 4, and 5 (Fig. 8). For the same engine block, entropy and contrast increase and correlation decreases with the increase of pixel distance. The reason is that the distribution of two concurrence pixels for larger pixel distance becomes more disordered and less correlated. However, for all the nine engine blocks, entropy, contrast, and correlation show a similar trend with various pixel distances. Therefore, pixel distance equal to one is suggested for surface face milling, when the spatial and height information of two adjacent pixels in all the four directions is of most concern. Moreover, if the machined surface has highly periodic feed marks, such as turned surfaces, a power spectral density technique could be used to choose the proper pixel distance [19].

A more detailed analysis of the results showed that entropy increased with flatness for the nine blocks except Block 6 and Block 8. For those surfaces with flatness more than $40 \mu\text{m}$ (Blocks 5 to

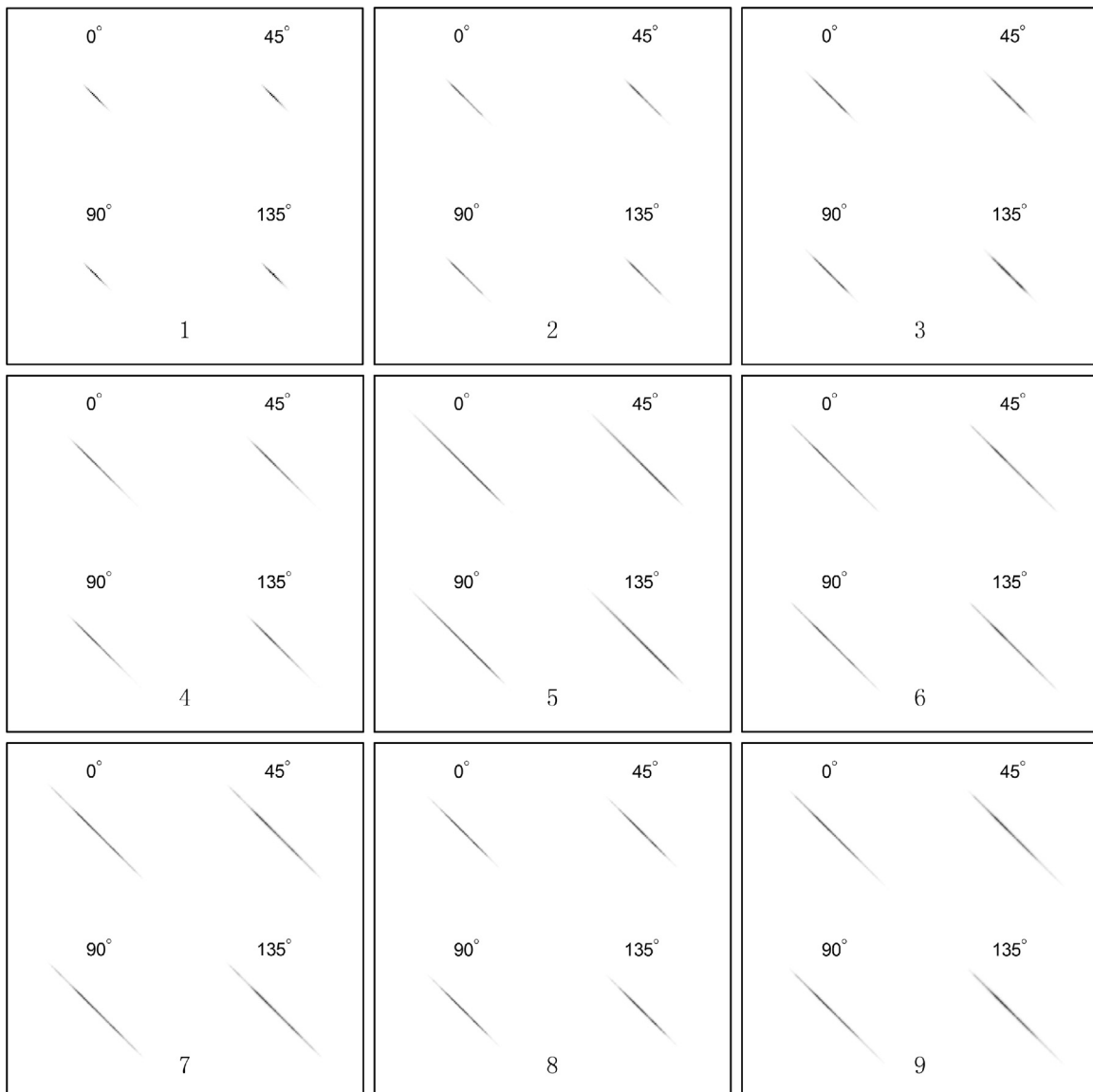


Fig. 7. GLCMs of Block 1 to Block 9 with pixel distance of 1.

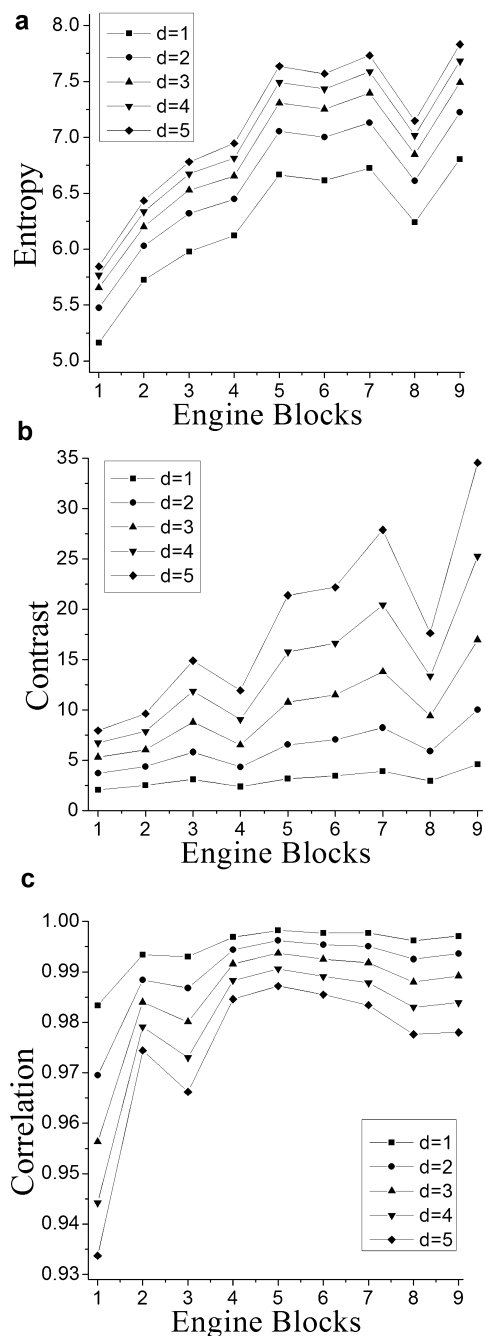


Fig. 8. GLCM characteristics of Block 1 to Block 9 with pixel distance equal to 1, 2, 3, 4, and 5: (a) entropy, (b) contrast, and (c) correlation.

Block 9), Block 8 had the least random height distribution. Thus, we can predict that Block 8 has different functional properties in certain areas with respect to Block 5, 6, 7, and 9. Contrast also showed a correlation with flatness except Block 4 and Block 8. The relatively lower contrast of Block 4 and 8 implied that surface form error of Block 4 and 8 were more likely caused by global deviations of the entire surface than local deviations. This implies that engineers can make systematic adjustment to the corresponding production line that manufactured Block 4 and 8. Correlation showed weak correlation with flatness but could be used to distinguish surface processing methods such as milling, turning, and grinding. Correlation of all the nine face-milled parts was high because each pixel was neighbored by another pixel with a similar gray level with pixel distance equal to one.

4. Conclusions and future work

This paper has developed an evaluation method for 3D surface form error using high definition metrology. An HDM data preprocessing method is proposed to convert millions of three dimensional data points into a height-encoded and position-maintained gray image. The height information (Z coordinates) is converted to pixel gray intensities, and the spatial information (X and Y coordinates) is converted to the pixel index. Then a modified GLCM is adopted to evaluate 3D surface form error using the converted gray image. Gray level of 256 and pixel distance of one are suggested when calculating GLCMs for machined surface. Entropy, contrast and correlation are calculated as an average of GLCM in four directions 0° , 45° , 90° , and 135° . Entropy indicates randomness of the surface height distribution and it is proportional to flatness. Contrast measures the degree of surface local deviation, which is the amount of local surface height difference between a pixel and its neighbor over the image. Correlation reflects the degree of how correlated a pixel is to another pixel in certain a direction and distance. These characteristics, including entropy, contrast and correlation, are complementary to surface flatness and provide a comprehensive evaluation of 3D surface form error. Moreover, these characteristics help engineers in better understanding of the surface quality from various angles and making due adjustment of the process.

Starting from 3D surface form error evaluation, three directions of further research are outlined. First, latest image analysis methods should be studied to evaluate 3D form error using HDM data. Second, 3D surface form error can be extended to machining process diagnosis, such as the wear of wiper insert in face milling and erroneous fixation of tool or part. Third, the relation of 3D surface form error and surface functional properties should be studied. For example, flatness is required to prevent the potential leakage of combustion gas, coolant and lubricant in the mating surfaces of engine blocks and engine heads. However, sometimes leakage may still happen with qualified flatness. Therefore, 3D surface form error characteristics could have more potentials than flatness to describe the sealing performance.

Acknowledgments

This work is supported by the National Natural Science Foundation of China (51075277 and 51275558), the National Science & Technology Pillar Program of China (2012BAF06B03), the Fund for Innovative Research Groups of the National Natural Science Foundation of China (51121063), the Program of Introducing Talents of Discipline to Universities (B06012), and Program for New Century Excellent Talents in University (NCET-11-0328).

References

- [1] Jiang X, Scott PJ, Whitehouse DJ, Blunt L. Paradigm shifts in surface metrology. Part II. The current shift. *Proceedings of the Royal Society A* 2007;463: 2071–99.
- [2] Pedonea P, Romanob D. Designing small samples for form error estimation with coordinate measuring machines. *Precision Engineering* 2011;35:262–70.
- [3] Huang Z, Shih AJ, Ni J. Laser interferometry hologram registration for three-dimensional precision measurements. *ASME Journal of Manufacturing Science and Engineering* 2006;128:1006–13.
- [4] 25178-6:2010 I, Geometrical Product Specifications (GPS) – Surface Texture: Areal – Part 6: Classification of methods for measuring surface texture; 2010.
- [5] Dong WP, Sullivan PJ, Stout KJ. Comprehensive study of parameters for characterising three-dimensional surface topography. I. Some inherent properties of parameter variation. *Wear* 1992;159:161–71.
- [6] Dong WP, Sullivan PJ, Stout KJ. Comprehensive study of parameters for characterising three-dimensional surface topography. II. Statistical properties of parameter variation. *Wear* 1993;167:9–21.
- [7] Dong WP, Sullivan PJ, Stout KJ. Comprehensive study of parameters for characterising three-dimensional surface topography. III. Parameters for characterising amplitude and some functional properties. *Wear* 1994;178:29–43.

- [8] Dong WP, Sullivan PJ, Stout KJ. Comprehensive study of parameters for characterising three-dimensional surface topography. IV. Parameters for characterising spatial and hybrid properties. *Wear* 1994;178:45–60.
- [9] 25178-2:2012 I, Geometrical Product Specifications (GPS) – Surface Texture: Areal – Part 2: Terms, definitions and surface texture parameters; 2012.
- [10] Liao Y, Stephenson DA, Ni J. A multifeature approach to tool wear estimation using 3D workpiece surface texture parameters. *ASME Journal of Manufacturing Science and Engineering* 2010;132:061008.
- [11] Li YQ, Ni J. B-spline wavelet-based multiresolution analysis of surface texture in end-milling of aluminum. *ASME Journal of Manufacturing Science and Engineering* 2011;133:011014.
- [12] Tai BL, Stephenson DA, Shih AJ. Improvement of surface flatness in face milling based on 3-D holographic laser metrology. *International Journal of Machine Tools & Manufacture* 2011;51:483–90.
- [13] Suriano S, Wang H, Hu SJ. Sequential monitoring of surface spatial variation in automotive machining processes based on high definition metrology. *Journal of Manufacturing Systems* 2012;31:8–14.
- [14] Lee DT, Schachter BJ. Two algorithms for constructing a Delaunay triangulation. *International Journal of Parallel Programming* 1980;9:219–42.
- [15] Haralick RM, Shanmugam K, Dinstein IH. Textural features for image classification. *IEEE Transactions on Systems, Man and Cybernetics* 1973;3: 610–21.
- [16] Baraldi A, Parmiggiani F. An investigation of the textural characteristics associated with gray level cooccurrence matrix statistical parameters. *IEEE Transactions on Geoscience and Remote Sensing* 1995;33:293–304.
- [17] Tien CL, Lyu YR, Jyu SS. Surface flatness of optical thin films evaluated by gray level co-occurrence matrix and entropy. *Applied Surface Science* 2008;254: 4762–7.
- [18] Tien CL, Lyu YR. Optical surface flatness recognized by discrete wavelet transform and grey level cooccurrence matrix. *Measurement Science and Technology* 2006;17:2299–305.
- [19] Dutta S, Datta A, Chakladar ND, Pal SK, Mukhopadhyay S, Sen R. Detection of tool condition from the turned surface images using an accurate grey level co-occurrence technique. *Precision Engineering* 2012;36:458–66.